IMAGING MASS SPECTROMETRY REVEALED THE PRODUCTION OF LYSO-PHOSPHATIDYLCHOLINE IN THE INJURED ISCHEMIC RAT BRAIN

Neuroscience 168 (2010) 219–225

IMAGING MASS SPECTROMETRY REVEALED THE PRODUCTION OF LYSO-PHOSPHATIDYLCHOLINE IN THE INJURED ISCHEMIC RAT BRAIN

S. KOIZUMI,[a] S. YAMAMOTO,[b] T. HAYASAKA,[c] Y. KONISHI,[c] M. YAMAGUCHI-OKADA,[a] N. GOTO-INOUE,[c] Y. SUGIURA,[c,d] M. SETOU[c]* AND H. NAMBA[a]

[a]*Department of Neurosurgery, Hamamatsu University School of Medicine, 1-20-1 Handayama, Higashi-ku, Hamamatsu, Shizuoka 431-3192, Japan*

[b]*Photon Medical Research Center, Hamamatsu University School of Medicine, 1-20-1 Handayama, Higashi-ku, Hamamatsu, Shizuoka 431-3192, Japan*

[c]*Department of Molecular Anatomy, Hamamatsu University School of Medicine, 1-20-1 Handayama, Higashi-ku, Hamamatsu, Shizuoka 431-3192, Japan*

[d]*Department of Bioscience and Biotechnology, Tokyo Institute of Technology, 4259 Nagatusuta-cho, Midori-ku, Yokohama, Kanagawa 226-8501, Japan*

Abstract—To develop an effective neuroprotective strategy against ischemic injury, it is important to identify the key molecules involved in the progression of injury. Direct molecular analysis of tissue using mass spectrometry (MS) is a subject of much interest in the field of metabolomics. Most notably, imaging mass spectrometry (IMS) allows visualization of molecular distributions on the tissue surface. To understand lipid dynamics during ischemic injury, we performed IMS analysis on rat brain tissue sections with focal cerebral ischemia. Sprague–Dawley rats were sacrificed at 24 h after middle cerebral artery occlusion, and brain sections were prepared. IMS analyses were conducted using matrix-assisted laser desorption/ionization time-of-flight mass spectrometer (MALDI-TOF MS) in positive ion mode. To determine the molecular structures, the detected ions were subjected to tandem MS. The intensity counts of the ion signals of *m*/*z* 798.5 and *m*/*z* 760.5 that are revealed to be a phosphatidylcholine, PC (16:0/18:1) are reduced in the area of focal cerebral ischemia as compared to the normal cerebral area. In contrast, the signal of *m*/*z* 496.3, identified as a lyso-phosphatidylcholine, LPC (16:0), was clearly increased in the area of focal cerebral ischemia. In IMS analyses, changes of PC (16:0/18:1) and LPC (16:0) are observed beyond the border of the injured area. Together with previous reports—that PCs are hydrolyzed by phospholipase A_2 (PLA_2) and produce LPCs,—our present results suggest that LPC (16:0) is generated during the injury process after cerebral ischemia, presumably via PLA_2 activation, and that PC (16:0/18:1) is one of its precursor molecules.

Key words: brain imaging, focal ischemia, imaging mass spectrometry, lyso-phosphatidylcholine.

*Corresponding author. Tel: +81-53-435-2292; fax: +81-53-435-2292.
E-mail address: setou@hama-med.ac.jp (M. Setou).

Abbreviations: AA, arachidonic acid; ADU, arbitrary decision units; CID, collision-induced dissociation; Da, daltons; DHB, 2,5-dihydroxybenzoic acid; ECs, endothelial cells; H, proton; HE, Hematoxylin-and-Eosin; IMS, imaging mass spectrometry; K, potassium; LPC, lyso-phosphatidylcholine; MALDI, matrix-assisted laser desorption/ionization; MALDI-TOF MS, matrix-assisted laser desorption/ionization time-of-flight mass spectrometer; MCA, middle cerebral artery; MCAO, MCA occlusion; MS, mass spectrometry; MS^n, tandem MS; m/z, mass-to-charge ratios; NL, neutral losses; Ox-LDL, oxidized low-density lipoprotein; PC, phosphatidylcholine; PLA2, phospholipase A2; PLC, phospholipase C; ROI, region of interest; TFA, trifluoroacetic acid; TOF, time-of-flight.

The progression of ischemic injury has been thought to involve many molecular pathways that play roles in the death of neurons. The molecular dynamics following ischemia is yet to be elucidated. Lipids play fundamental roles in the maintenance of cell structure and in mediating cell signaling. Considering that the brain is one of the most lipid-rich organs, with accounting for approximately 50% of dry weight (Trim et al., 2008), it has been suggested that they play fundamental roles in various brain functions. Nonetheless, lipid distributions in the brain during the progression of ischemia remain largely unknown, due to the limitations of imaging methods used to visualize the tissue distributions of lipids.

Direct molecular analysis of biological tissue using mass spectrometry (MS) provides valuable information (Sugiura and Setou, 2010). Imaging mass spectrometry (IMS) of biological tissues, using matrix-assisted laser desorption/ionization (MALDI), is an especially powerful tool for visualizing the distributions of various molecules(Harada et al., 2009), and is thus applicable to the imaging of bio-molecules (Stoeckli et al., 2001; Kimura et al., 2009), biomarker discovery (Morita et al., 2010; Zaima et al., 2009) and drug delivery (Reyzer et al., 2003) in tissues. IMS can separate multiple lipids according their mass-to-charge ratios (*m*/*z*), and visualize the tissue distribution of each molecule (Hayasaka et al., 2008; Sugiura and Setou, 2010). Furthermore, the use of tandem MS (MS^n) allows identification of the structures of the visualized molecules (Hayasaka et al., 2009).

In this study, we used IMS to visualize lipid distributions in rat brain tissues during focal cerebral ischemia. Our present results reveal dynamic conversion from phosphatidylcholine (PC) to lyso-phosphatidylcholine (LPC) in brain areas with ischemic injury.

EXPERIMENTAL PROCEDURES

Animals and surgery

All experiments were performed according to the rules of animal experimentation and the guide for the care and use of laboratory animals of Hamamatsu University School of Medicine. Eight weeks old Sprague–Dawley rats (290–310 g) purchased from

0306-4522/10 $ - see front matter
doi:10.1016/j.neuroscience.2010.03.056

SLC Inc. (Hamamatsu, Japan) were fed lab chow *ad libitum* and maintained in a thermally controlled (27 °C), 12 h light/dark cycle environment. The rats were anesthetized with 1.3%–1.8% isoflurane by nasopharyngeal insufflations under spontaneous respiration (Abbott Japan Co., Ltd., Tokyo, Japan) (Yamasaki et al., 2003). Temperature was maintained at 37 °C throughout the procedure using rectal temperature regulating heating pad. The left middle cerebral artery (MCA) was exposed and cauterized distal to the lenticulostriatal branches by a modification of the method of Tamura et al. (Tamura et al., 1981; Yamamoto et al., 1988).

Preparation of tissue samples

The rats were sacrificed at 24 h after MCA occlusion (MCAO) under deep anesthesia and then decapitated. The brains were then dissected. Immediately after dissection, the rat brains were flash frozen in liquid hexane and stored at −20 °C. Tissues were sliced at a 7 μm thickness with a cryostat (CM1950; Leica, Wetzler, Germany), placed directly onto MALDI plate inserts, and stored at −20 °C until matrix application and subsequent IMS analysis. The adjacent brain section, also 20 μm in thickness, was used for counter staining with Hematoxylin-and-Eosin (HE). The MALDI matrix 2,5-dihydroxybenzoic acid (DHB) was purchased from Bruker Daltonics (Leipzig, Germany). Bradykinin and angiotensin-II were obtained from Sigma-Aldrich, Japan (Tokyo, Japan) and used as calibration standards. Trifluoroacetic acid (TFA) was purchased from Kanto Chemical Company (Tokyo, Japan). Methanol was purchased from Wako Pure Chemical Industries (Osaka, Japan).

IMS analyses and identification of phospholipids

In total, 0.5 ml of DHB matrix solution (30 mg/mL in 70% methanol/0.1% TFA) were sprayed onto the tissue as previously described (Schwartz et al., 2003; Shimma et al., 2008). After drying, MALDI plate inserts were installed in the ionization chamber. MS and IMS analyses were acquired using a quadrupole time-of-flight (TOF) tandem mass spectrometer (QSTAR XL, Applied Biosystems/MDS Sciex, Thornhill, ON, Canada) in positive ion mode. The mass spectra were calibrated externally using a standard peptide calibration mixture containing a bradykinin peptide fragment (amino acid residues 1–7) and a human angiotensin-II peptide fragment (amino acid residues 18–39).

For IMS, the raster scan was performed automatically. The laser was used at energy of 40% (4.0 μJ) and a repetition rate of 100 Hz. Mass spectra were acquired with the laser firing for approximately 2.55 s per spot. The interval of data points was 200 μm, yielding a total of approximately 4500 data points. Mass spectrometric data were averaged at each analytical point, such as contralateral hemisphere and ipsilateral hemisphere, within the region of interest (ROI) and shown as mass spectra. For three specific peaks, the ion signals were accumulated and compared among contralateral hemisphere and ipsilateral hemisphere. Then, all mass spectrometric data were converted to apply the Biomap ion imaging software (Novartis, Basel, Switzerland) using software provided by Applied Biosystems/MDS Sciex. All ion images were processed using BioMap. And to examine the dynamics of the ion signals and HE staining signals at the ischemic border, Scion Image (http://www.scioncorp.com/) were used. To quantify the signal intensities of the ion signals and HE staining signals, ADU (arbitrary decision units) were used provided from Scion Image.

In MS/MS analysis, the instrument settings were changed to correspond to the ions from the molecules of interest. The laser energy and collision-induced dissociation (CID) settings were adjusted from 40% to 60% and from 200 to 400, respectively. The mass spectra were obtained from either contralateral hemisphere or ipsilateral hemisphere and accumulated. Lipid databases, such as LIPID MAPS (http://www.lipidmaps.org/) and the Lipid Search (http://lipidsearch.jp/), were used to determine the structure of lipid molecules.

Data quantification and statistical analysis

All but the MS/MS data were obtained from a single scan of an ischemic brain section. The intensities of ion signals were measured at several analytical points within the ROI, and the compiled data were expressed as means±SE or means±SD. Statistical analyses were performed using the Student's *t*-test for 2-group comparisons. Differences were considered to be significant at $P<0.05$.

RESULTS

Direct MS analysis of ischemic brain tissue

Fig. 1 shows mass spectra obtained from rat cerebral cortical hemispheres contralateral (normal, Fig. 1a) and ipsilateral (ischemic, Fig. 1b) to MCAO. Each analytical point is indicated by a blue point on HE-stained images of adjacent sections (insets). There is no injury in the contralateral hemisphere, whereas in the ipsilateral hemisphere, tissue degeneration around the analytical point is apparent (Fig. 1a, b). Signals at *m*/*z* 798.5, are predominantly detected in normal brain areas as reported previously. In the ischemic brain area, the ion signal of *m*/*z* 798.5 is substantially reduced (Fig. 1b). In contrast, there were several ion signals in the lower mass range. For example, Signals at *m*/*z* 496.3 (Fig. 1b) was clearly increased in the ischemic area.

Structure determinations of PC and LPC by MS/MS analyses

MS/MS analyses were performed to determine the structure of peaks at *m*/*z* 798.5 and *m*/*z* 496.3 (Fig. 2). From the precursor ion at *m*/*z* 798.5, the product ions at *m*/*z* 739.5, *m*/*z* 615.4, and *m*/*z* 577.5 were detected (Fig. 2a). The difference between the mass values represents neutral losses (NL) corresponding to 59, 124, and 38 Daltons (Da). These NLs of 59 and 124 Da are known to represent, respectively, trimethylamine [$N(CH_3)_3$], the cyclophosphane ring [$(CH_2)_2PO_4H$], all of which are the parts of the PC species. The NL of 38 Da corresponds to the replacement of adduct ion to PC from potassium (K) to proton (H). These NLs have been shown to be detectable by MS/MS analysis of potassium-adducted PC species (Hsu and Turk, 2003; Pulfer and Murphy, 2003). The product-ion spectrum even indicated peaks at *m*/*z* 184.1 and *m*/*z* 163.0. These peaks correspond to the headgroup $(CH_3)_3N(CH_2)_2PO_4H$; trimethylamine and the cyclophosphane ring of PC and [cyclophosphane ring+K]$^+$ from the headgroup, respectively. The database search of the LIPID MAPS as well as previous studies (Hsu et al., 1998; Hsu and Turk, 2003; Pulfer and Murphy, 2003) have suggested that the ion at *m*/*z* 798.5 is [PC (34:1)+K]$^+$. The NL of fatty acids from alkali-metal adducted PC species has reportedly been identified by electrospray ionization-MS/MS analysis (Jackson et al., 2007). MS/MS analyses using our IMS system were able to detect the product ion at *m*/*z* 542.2 that represents the NL of the fatty acid (16:0) from the precursor ion of *m*/*z* 798.5. Therefore,

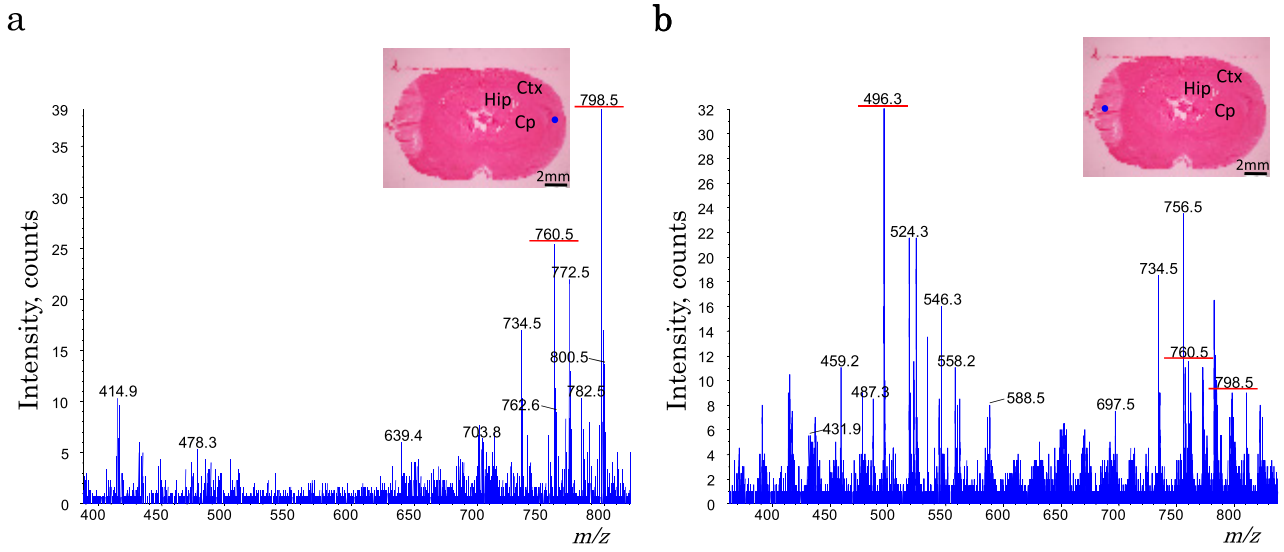

Fig. 1. Direct mass analysis of rat brain tissue after MCAO. Mass spectra obtained from a rat ischemic brain section using a quadrupole-TOF tandem mass spectrometer with QSTAR XL in positive ion mode. HE staining of the adjacent section is shown in the insets to indicate the injured area and analytical points (blue points). Data from the normal cerebral area (a) and the focal cerebral ischemic area (b) are shown in the range of 400 to 800. Numbers above ion peaks indicate their *m*/*z* values. Cp, caudate putamen; Ctx, cerebral cortex; HP, hippocampus.

the ion at *m*/*z* 798.5 can be identified in detail as potassium-adducted PC (16:0/18:1). Similarly, the ion at *m*/*z* 760.5 can be identified in detail as proton-adducted PC (16:0/18:1) (Data not shown). And, from the precursor ion at *m*/*z* 496.3, the product ions at *m*/*z* 184.1 and *m*/*z* 313.3 were detected (Fig. 2b). An NL of 183 Da from the precursor ion corresponds to the headgroup. So, the fragment peaks at *m*/*z* 184.1 and *m*/*z* 313.3 correspond to $[PC\ headgroup+H]^+$ and an NL of 183 Da from a precursor peak, respectively. The product-ion spectrum even indicated peaks at *m*/*z* 104.1 and *m*/*z* 125.0.

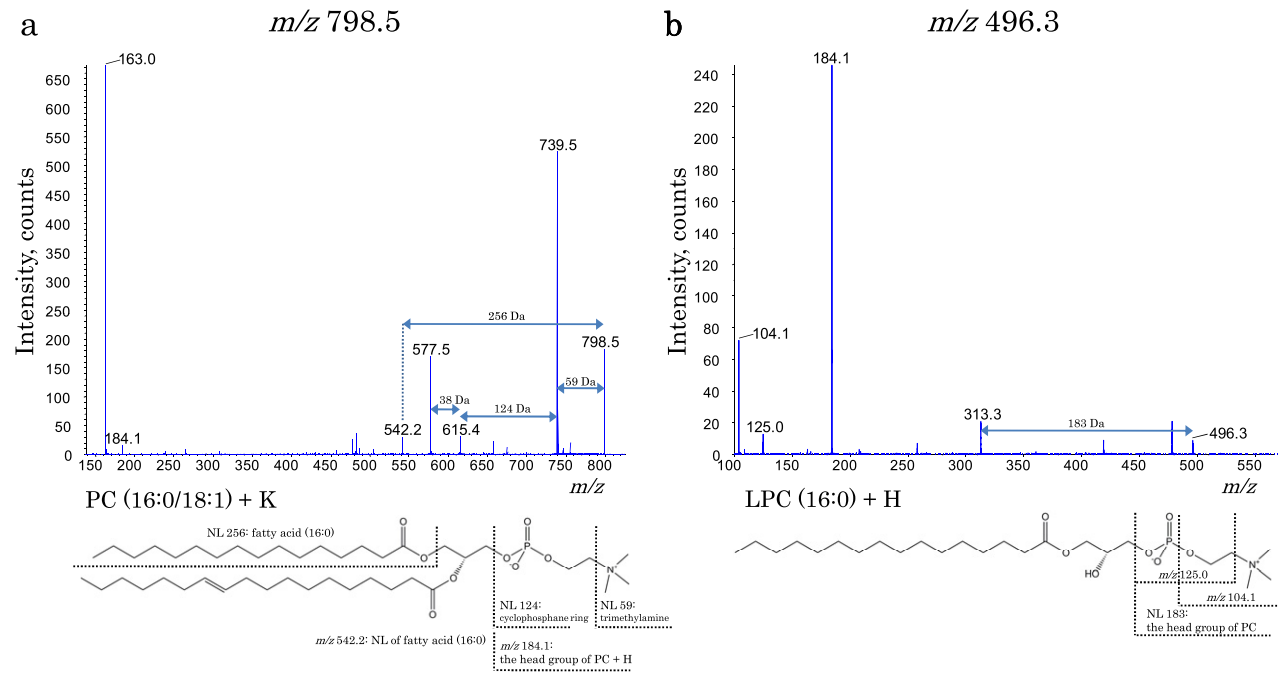

Fig. 2. MS/MS analyses of ions responsive to brain ischemia. The precursor ions at *m*/*z* 798.5 and *m*/*z* 496.3 were subjected to MS/MS analysis. Spectra of product ions (top) and the determined structures (bottom) are shown. (a) From product ions of *m*/*z* 798.5, NLs corresponding to trimethylamine [$N(CH_3)_3$, 59 Da], the cyclophosphane ring ($(CH_2)_2PO_4H$, 124 Da) and the replacement of adduct ion from potassium to proton (K, 39 Da; H, 1 Da) were observed. The product ion at *m*/*z* 542.2 corresponding to an NL of a fatty acid (16:0) was also detected. (b) From product ions of *m*/*z* 496.3, an NL corresponding to the headgroup ($(CH_3)_3N(CH_2)_2PO_4H$; trimethylamine and the cyclophosphane ring) was observed. From a subsequent database search, ions at *m*/*z* 798.5 and 496.3 were identified as $[PC\ (16:0/18:1)+K]^+$ and $[LPC\ (16:0)+H]^+$, respectively. For interpretation of the references to color in this figure legend, the reader is referred to the Web version of this article.

These peaks correspond to $[(CH_3)_3N(CH_2)_2O+H]^+$ and [cyclophosphane ring+H]$^+$ from the headgroup, respectively. From the results of the database search, we identified the ion at *m*/*z* 496.3 as proton-adducted LPC (16:0).

Amounts of PC (16:0/18:1) and LPC (16:0) altered in the ischemic area

To quantify the ion signals, we measured ion intensities at analytical points within the ROI in five different rats. We observed the ion intensity of potassium-adducted PC (16:0/18:1) (*m*/*z* 798.5) to be relatively low in the focal ischemic area as compared with the control area (left columns in Fig. 3a). Similarly, the ion intensity of *m*/*z* 760.5 corresponding to the proton-adducted PC (16:0/18:1) was also lower in the ischemic area (right columns in Fig. 3a). In contrast, the ion intensity of proton-adducted LPC (16:0) (*m*/*z* 496.3) was higher in the ischemic area than in the control area (Fig. 3b).

Distribution analysis of PC (16:0/18:1) and LPC (16:0) in ischemic rat brain by IMS

Next, we visualized the distributions of ion signals in brain tissues. In the contralateral hemisphere at 24 h after MCAO, the ion intensities of PC (16:0/18:1) (*m*/*z* 798.5 and *m*/*z* 760.5) were abundantly detected throughout the cerebral cortex (Fig. 4a, b), as reported previously (Jackson et al., 2005, 2007). In contrast, these ions were exclusively distributed in areas of degeneration in the ipsilateral hemisphere (Fig. 4a, b). Remarkably, the ion distribution of *m*/*z* LPC (16:0) (*m*/*z* 496.3) was specifically restricted to the area of degeneration in which PC (16:0/18:1) was reduced (Fig. 4c). As a merged image (Fig. 4d), ion signals of PC (16:0/18:1) and LPC (16:0) are indicated by blue and red, respectively. We also collected the IMS data at 20 h after MACO. At this time point, we detected only a slight LPC induction at a restricted area in the ipsilateral hemisphere (Fig. 4e, f).

We speculate that cells at the border of the injured area are undergoing degeneration. To examine the PC dynamics in these cells, the ion signals of PC (16:0/18:1) and LPC (16:0) were plotted across the border from the ischemic area to the normal area (Fig. 4g). The ion signals of PC (16:0/18:1) (*m*/*z* 798.5 and *m*/*z* 760.5) were gradually increased until reach to a plateau in the control region whereas the signal of LPC (16:0) (*m*/*z* 496.3) was complementally decreased (Fig. 4g). The signal plot of HE staining revealed the border of the degenerative zone to be localized between 0.8 and 0.9 mm from the starting point. Signal changes of PC (16:0/18:1) and LPC (16:0) due to ischemia were observed at the border, and points even further from the ischemic border (i.e. 0.9–1.1 mm from the starting point) (Fig. 4g). These observations raise the possibility that amount of LPCs are increased not only in the ischemic core, but also in the ischemic penumbra area in which cells are undergoing degeneration.

DISCUSSION

In the present study, we analyzed ischemic rat brain sections using direct mass spectrometry, and found LPC (16:0) to be induced in the injured area following MCAO, whereas PC (16:0/18:1) was reduced complementally in the ischemic area. Previous studies have suggested that PC can be hydrolyzed by phospholipase A_2 (PLA_2) at the *sn*-2 position to generate LPC and free fatty acid (Steinbrecher and Pritchard, 1989). These observations raise the possibility that LPC (16:0) might be produced from PC (16:0/18:1) in the focal ischemic area. Consistently, it has reported that ischemic damage cause a Ca^{2+}-dependent activation of PLA_2 via NMDA receptor stimulation (Lee et al., 2000), and mice lacking cytosolic PLA_2 is partially protected from the effect of MCAO (Bonventre et al., 1997). Furthermore, a remarkable induction of cytosolic PLA_2 was reported in the dorsal hippocampal cytosolic extracts after global forebrain ischemia (Clemens et al.,

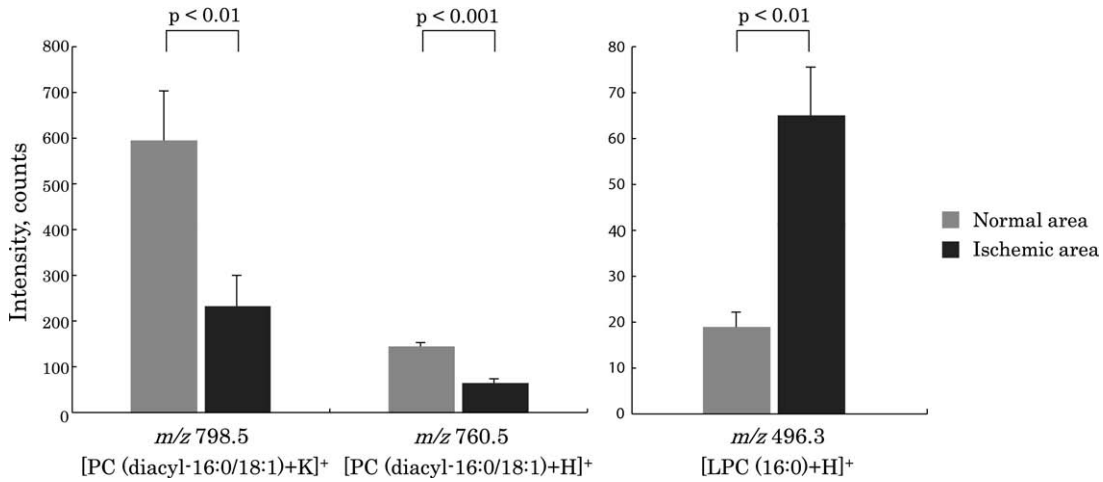

Fig. 3. Amounts of PC (16:0/18:1) and LPC (16:0) altered after brain ischemia. The ion intensities corresponding to (a, left) [PC (16:0/18:1)+K]$^+$ (*m*/*z* 798.5), (a, right) [PC (16:0/18:1)+H]$^+$ (*m*/*z* 760.5) and (b) [LPC (16:0)+H]$^+$ (*m*/*z* 496.3) were quantified. Data were obtained from five different rats in each normal or ischemic area, and expressed as means±SE. In the ischemic brain area, ion signals corresponding to PC (16:0/18:1) were decreased whereas those of LPC (16:0) showed marked induction.

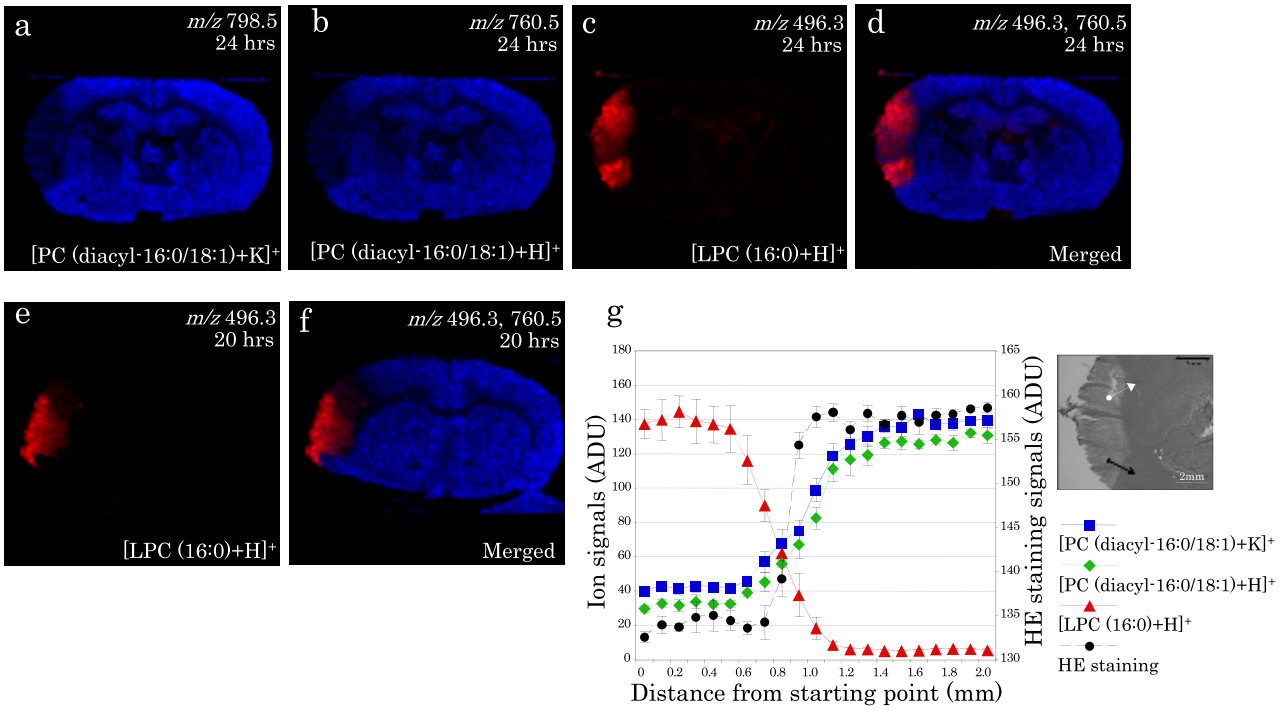

Fig. 4. Distributions of PC (16:0/18:1) and LPC (16:0) in the ischemic brain. (a–d) Distributions of $[PC\ (16:0/18:1)+K]^+$ (a), $[PC\ (16:0/18:1)+H]^+$ (b) and $[LPC\ (16:0)+H]^+$ (c) in the ischemic brain at 24 h after MCAO as well as a merged image (d) are presented. In (d), ion signals of $[PC\ (16:0/18:1)+H]^+$ and $[LPC\ (16:0)+H]^+$ are indicated by blue and red, respectively. (e, f) Distributions of $[LPC\ (16:0)+H]^+$ (e) in the ischemic brain at 20 h after MCAO as well as a merged image (f) are presented. In (f), ion signals of $[PC\ (16:0/18:1)+H]^+$ and $[LPC\ (16:0)+H]^+$ are indicated by blue and red, respectively. (g) The intensities of each ion were plotted across the border from the ischemic area to the normal area, as indicated. The inset indicates the measured area on the adjacent section stained by HE. To indicate the border of the injured area, the HE staining signals at the corresponding position were also quantified and plotted on the graph. Data were corrected from five adjacent zones and the normalized intensities are presented as means±SD.

1996). We detected only a slight induction of cytosolic PLA_2 by Western blotting of cerebral hemisphere at 24 h after MCAO (data not shown). It might be possible that induction of cytosolic PLA_2 occurs at a restricted area in our system, thus hard to detect by using lysates prepared from whole cerebral hemisphere. Alternatively, there might be some molecular mechanisms (e.g. reacylation rate to become PCs, Shindou and Shimizu, 2009), involved in the LPC induction in MCAO.

Apart from the mechanisms by which LPCs are induced in ischemia, the roles of LPCs in the progression of ischemic injury have not been elucidated. In our IMS, LPC (16:0) was detected in a restricted area at 20 h after MCAO and was distributed in larger ischemic area by 24 h (Fig. 4). In addition, the region surrounding this area showed induction of LPC at least in some extent. We speculate that LPCs are induced not only in the ischemic core, but also in the ischemic penumbra area. Our present observations raise the possibility that production of LPCs participates in the progression of brain injury in the setting of brain ischemia. In future, it will be important to compare IMS image with diffusion- and perfusion-weighted magnetic resonance imaging to compare the expansion of the injury and induction of molecules (Reith et al., 1995; Nagel et al., 2004).

Outside of the nervous system, LPCs are suggested to play important roles in atherosclerosis and inflammatory diseases by altering the functions of various cell-types, including endothelial cells (ECs), smooth muscle cells, monocytes, macrophages, and T-cells. LPCs also participate in disturbances of vascular tone (Miwa et al., 1997), promoting cytokine effects (Murugesan et al., 2003), regulation of adhesion and chemoattraction (Thukkani et al., 2003), induction of apoptosis (Takahashi et al., 2002), induction of reactive oxygen species (Matsubara and Hasegawa, 2005) and reduction of nitric oxides (Deckert et al., 1998). Furthermore, LPC has been identified as a major phospholipid component of oxidized low-density lipoprotein (Ox-LDL) which is a key factor in arteriosclerosis development (Witztum and Steinberg, 1991; Matsumoto et al., 2007). Thus, LPC is regarded as a risk factor for vascular endothelial function damage, as is Ox-LDL. In myocardial tissues, LPCs accumulate in intra- and extracellular spaces via increments in PLA_2 during ischemia, and play an important role in the development of ischemia-reperfusion injury (Watanabe and Okada, 2003). In similar ways, LPCs might also play roles in focal cerebral ischemic injury.

Upon PLA_2 activation, PCs are converted to LPCs and fatty acids (Murakami et al., 1997). It could involves rapid release of free arachidonic acid (AA) (Busto et al., 1989) and the induction of eicosanoids from AA (Miettinen et al., 1997) which regulate neuronal degeneration (Gaudet and Levine, 1979; Iannotti et al., 1981; Bhakoo et al., 1984). In

addition, other molecular change should exist in earlier stage of ischemia progression. Although we are not able to detect these bio-molecules in our current system, development of IMS technique in near future could provide further information.

Acknowledgments—This research is supported in part by Japan Science and Technology Agency grants SENTAN, JST and Japan Society for the Promotion of Science grants WAKATE-S to Mitsutoshi Setou.

REFERENCES

Bhakoo KK, Crockard HA, Lascelles PC, Avery SF (1984) Prostaglandin synthesis and oedema formation during reperfusion following experimental brain ischaemia in the gerbil. Stroke 15:891–895.

Bonventre JV, Huang Z, Taheri MR, O'Leary E, Li E, Moskowitz MA, Sapirstein A (1997) Reduced fertility and postischaemic brain injury in mice deficient in cytosolic phospholipase A2. Nature 390:622–625.

Busto R, Globus MY, Dietrich WD, Martinez E, Valdes I, Ginsberg MD (1989) Effect of mild hypothermia on ischemia-induced release of neurotransmitters and free fatty acids in rat brain. Stroke 20: 904–910.

Clemens JA, Stephenson DT, Smalstig EB, Roberts EF, Johnstone EM, Sharp JD, Little SP, Kramer RM (1996) Reactive glia express cytosolic phospholipase A2 after transient global forebrain ischemia in the rat. Stroke 27:527–535.

Deckert V, Brunet A, Lantoine F, Lizard G, Millanvoye-van Brussel E, Monier S, Lagrost L, David-Dufilho M, Gambert P, Devynck MA (1998) Inhibition by cholesterol oxides of NO release from human vascular endothelial cells. Arterioscler Thromb Vasc Biol 18:1054–1060.

Gaudet RJ, Levine L (1979) Transient cerebral ischemia and brain prostaglandins. Biochem Biophys Res Commun 86:893–901.

Harada T, Yuba-Kubo A, Sugiura Y, Zaima N, Hayasaka T, Goto-Inoue N, Wakui M, Suematsu M, Takeshita K, Ogawa K, Yoshida Y, Setou M (2009) Visualization of volatile substances in different organelles with an atmospheric-pressure mass microscope. Anal Chem 81:9153–9157.

Hayasaka T, Goto-Inoue N, Zaima N, Kimura Y, Setou M (2009) Organ-specific distributions of lysophosphatidylcholine and triacylglycerol in mouse embryo. Lipids 44:837–848.

Hayasaka T, Goto-Inoue N, Sugiura Y, Zaima N, Nakanishi H, Ohishi K, Nakanishi S, Naito T, Taguchi R, Setou M (2008) Matrix-assisted laser desorption/ionization quadrupole ion trap time-of-flight (MALDI-QIT-TOF)-based imaging mass spectrometry reveals a layered distribution of phospholipid molecular species in the mouse retina. Rapid Commun Mass Spectrom 22:3415–3426.

Hsu FF, Turk J (2003) Electrospray ionization/tandem quadrupole mass spectrometric studies on phosphatidylcholines: the fragmentation processes. J Am Soc Mass Spectrom 14:352–363.

Hsu FF, Bohrer A, Turk J (1998) Formation of lithiated adducts of glycerophosphocholine lipids facilitates their identification by electrospray ionization tandem mass spectrometry. J Am Soc Mass Spectrom 9:516–526.

Iannotti F, Crockard A, Ladds G, Symon L (1981) Are prostaglandins involved in experimental ischemic edema in gerbils? Stroke 12:301–306.

Jackson SN, Wang HY, Woods AS (2005) Direct profiling of lipid distribution in brain tissue using MALDI-TOFMS. Anal Chem 77:4523–4527.

Jackson SN, Ugarov M, Egan T, Post JD, Langlais D, Albert Schultz J, Woods AS (2007) MALDI-ion mobility-TOFMS imaging of lipids in rat brain tissue. J Mass Spectrom 42:1093–1098.

Kimura Y, Tsutsumi K, Sugiura Y, Setou M (2009) Medical molecular morphology with imaging mass spectrometry. Med Mol Morphol 42:133–137.

Lee JM, Grabb MC, Zipfel GJ, Choi DW (2000) Brain tissue responses to ischemia. J Clin Invest 106:723–731.

Matsubara M, Hasegawa K (2005) Benidipine, a dihydropyridine-calcium channel blocker, prevents lysophosphatidylcholine-induced injury and reactive oxygen species production in human aortic endothelial cells. Atherosclerosis 178:57–66.

Matsumoto T, Kobayashi T, Kamata K (2007) Role of lysophosphatidylcholine (LPC) in atherosclerosis. Curr Med Chem 14:3209–3220.

Miettinen S, Fusco FR, Yrjanheikki J, Keinanen R, Hirvonen T, Roivainen R, Narhi M, Hokfelt T, Koistinaho J (1997) Spreading depression and focal brain ischemia induce cyclooxygenase-2 in cortical neurons through N-methyl-D-aspartic acid-receptors and phospholipase A2. Proc Natl Acad Sci U S A 94:6500–6505.

Miwa Y, Hirata K, Kawashima S, Akita H, Yokoyama M (1997) Lysophosphatidylcholine inhibits receptor-mediated Ca2+ mobilization in intact endothelial cells of rabbit aorta. Arterioscler Thromb Vasc Biol 17:1561–1567.

Morita Y, Ikegami K, Goto-Inoue N, Hayasaka T, Zaima N, Tanaka H, Uehara T, Setoguchi T, Sakaguchi T, Igarashi H, Sugimura H, Setou M, Konno H (2010) Imaging mass spectrometry of gastric carcinoma in formalin-fixed paraffin-embedded tissue microarray. Cancer Sci 101:267–273.

Murakami M, Nakatani Y, Atsumi G, Inoue K, Kudo I (1997) Regulatory functions of phospholipase A2. Crit Rev Immunol 17:225–283.

Murugesan G, Sandhya Rani MR, Gerber CE, Mukhopadhyay C, Ransohoff RM, Chisolm GM, Kottke-Marchant K (2003) Lysophosphatidylcholine regulates human microvascular endothelial cell expression of chemokines. J Mol Cell Cardiol 35:1375–1384.

Nagel S, Wagner S, Koziol J, Kluge B, Heiland S (2004) Volumetric evaluation of the ischemic lesion size with serial MRI in a transient MCAO model of the rat: comparison of DWI and T1WI. Brain Res Brain Res Protoc 12:172–179.

Pulfer M, Murphy RC (2003) Electrospray mass spectrometry of phospholipids. Mass Spectrom Rev 22:332–364.

Reith W, Hasegawa Y, Latour LL, Dardzinski BJ, Sotak CH, Fisher M (1995) Multislice diffusion mapping for 3-D evolution of cerebral ischemia in a rat stroke model. Neurology 45:172–177.

Reyzer ML, Hsieh Y, Ng K, Korfmacher WA, Caprioli RM (2003) Direct analysis of drug candidates in tissue by matrix-assisted laser desorption/ionization mass spectrometry. J Mass Spectrom 38:1081–1092.

Schwartz SA, Reyzer ML, Caprioli RM (2003) Direct tissue analysis using matrix-assisted laser desorption/ionization mass spectrometry: practical aspects of sample preparation. J Mass Spectrom 38:699–708.

Shimma S, Sugiura Y, Hayasaka T, Zaima N, Matsumoto M, Setou M (2008) Mass imaging and identification of biomolecules with MALDI-QIT-TOF-based system. Anal Chem 80:878–885.

Shindou H, Shimizu T (2009) Acyl-CoA:lysophospholipid acyltransferases. J Biol Chem 284:1–5.

Steinbrecher UP, Pritchard PH (1989) Hydrolysis of phosphatidylcholine during LDL oxidation is mediated by platelet-activating factor acetylhydrolase. J Lipid Res 30:305–315.

Stoeckli M, Chaurand P, Hallahan DE, Caprioli RM (2001) Imaging mass spectrometry: a new technology for the analysis of protein expression in mammalian tissues. Nat Med 7:493–496.

Sugiura Y, Setou M (2010) Imaging mass spectrometry for visualization of drug and endogenous metabolite distribution: toward in situ pharmacometabolomes. J Neuroimmune Pharmacol 5:31–43.

Takahashi M, Okazaki H, Ogata Y, Takeuchi K, Ikeda U, Shimada K (2002) Lysophosphatidylcholine induces apoptosis in human endothelial cells through a p38-mitogen-activated protein kinase-dependent mechanism. Atherosclerosis 161:387–394.

Tamura A, Graham DI, McCulloch J, Teasdale GM (1981) Focal cerebral ischaemia in the rat. 1. Description of technique and early neuropathological consequences following middle cerebral artery occlusion. J Cereb Blood Flow Metab 1:53–60.

Thukkani AK, McHowat J, Hsu FF, Brennan ML, Hazen SL, Ford DA (2003) Identification of alpha-chloro fatty aldehydes and unsaturated lysophosphatidylcholine molecular species in human atherosclerotic lesions. Circulation 108:3128–3133.

Trim PJ, Atkinson SJ, Princivalle AP, Marshall PS, West A, Clench MR (2008) Matrix-assisted laser desorption/ionisation mass spectrometry imaging of lipids in rat brain tissue with integrated unsupervised and supervised multivariant statistical analysis. Rapid Commun Mass Spectrom 22:1503–1509.

Watanabe M, Okada T (2003) Lysophosphatidylcholine-induced myocardial damage is inhibited by pretreatment with poloxamer 188 in isolated rat heart. Mol Cell Biochem 248:209–215.

Witztum JL, Steinberg D (1991) Role of oxidized low density lipoprotein in atherogenesis. J Clin Invest 88:1785–1792.

Yamamoto M, Tamura A, Kirino T, Shimizu M, Sano K (1988) Behavioral changes after focal cerebral ischemia by left middle cerebral artery occlusion in rats. Brain Res 452:323–328.

Yamasaki K, Kuroe K, Kamimura R (2003) A new method of inhalation anesthesia with nasopharyngeal insufflation in rat experiment. Exp Anim 52:349–351.

Zaima N, Matsuyama Y, Setou M (2009) Principal component analysis of direct matrix-assisted laser desorption/ionization mass spectrometric data related to metabolites of fatty liver. J Oleo Sci 58: 267–273.

(Accepted 23 March 2010)
(Available online 1 April 2010)